

The Multilegged Autonomous eXplorer (MAX)

Alberto Elfes, Ryan Steindl, Fletcher Talbot, Farid Kendoul, Pavan Sikka, Tom Lowe, Navinda Kottege, Marko Bjelonic, Ross Dungavell, Tirthankar Bandyopadhyay and Marcus Hoerger

Abstract—To address the goal of locomotion in very complex and challenging terrains, the authors are developing a new class of Ultralight Legged Robots. This paper presents the Multilegged Autonomous eXplorer (MAX), an ultralight, six-legged robot for exploration and traversal of difficult terrain. The design of MAX emphasizes a low mass/size ratio, high locomotion efficiency, and high payload capability compared to total system mass. MAX is 2.25 m tall when in a fully erect stance and has a mass of approximately 60 kg. This means that it is 5 to 20 times lighter than robots of comparable size. MAX is being used to explore modelling and control of Ultralight Legged Robots subject to flexing, oscillations and swaying; algorithms for gait planning and motion planning under uncertainty; and navigation planning for traversal of complex 3D terrains. The paper presents the design of MAX, provides an overview of the control system developed, summarizes results from indoor and outdoor tests, discusses system performance and outlines the challenges to be addressed next.

I. INTRODUCTION

Robot systems are increasingly being used in mining, agriculture, biosecurity, environmental monitoring, science surveys, defense, next-generation manufacturing, search and rescue, disaster recovery, and many others domains. While some missions can be executed using UAVs, ground robots are often required for *in situ* sensing of the deployment area and for actuation on objects in the environment of operation.

Current ground robots, however, are very limited in the type of terrain they can traverse. Estimates indicate that 30 - 50% of the Earth's land surface is not accessible to wheeled or tracked vehicles, because it is either too steep, too heavily vegetated, too cluttered or too marshy [1], [2].

Human beings and animals, on the other hand, have a remarkable ability to walk and run over a wide variety of natural and man-made terrain. Legged robots have hence been proposed as the solution to traversing difficult terrain; however, current systems, while promising, are far from adequate for extended field missions. Smaller legged robots are severely limited in payload and effective range; larger outdoor legged robots are often too inefficient and slow for field use, and unable to navigate really challenging terrain. Some of these problems are related to the intrinsic performance limitations of legged systems [3].

To address the goal of locomotion in very complex and challenging terrains, the authors are developing a new class of Ultralight Legged Robots (ULRs). The design of ULRs emphasizes low mass/size ratios, high locomotion efficiency, and high payload capability compared to total system mass.

The authors are with the Robotics and Autonomous Systems Research Group, CSIRO, Pullenvale, Brisbane, QLD 4069. Correspondence should be addressed to Alberto.Elfes@csiro.au.



Fig. 1. The Multilegged Autonomous eXplorer (MAX), an ultralight, six-legged robot with 18 DOFs. In a fully erect stance, MAX is 2.25 m tall; it is shown here in a cruise stance, with the body lower than the knees for greater stability.

This paper presents the Multilegged Autonomous eXplorer (MAX), our first prototype of an ultralight, six-legged robot for exploration and traversal of difficult terrain (Fig. 1). It is 2.25 m tall when in a fully erect stance and weighs approximately 60 kg. This means that it is 5 to 20 times lighter than robots of comparable size [4]. MAX is a research vehicle to explore modelling and control of Ultralight Legged Robots subject to flexing, oscillations and swaying; algorithms for gait planning and motion planning under uncertainty; and navigation planning for traversal of complex 3D terrains. The vehicle is comprehensively instrumented and carries ranging systems to map the 3D structure of the terrain being traversed by the robot. In this paper we present the design of MAX, provide an overview of the control system developed, summarize results from indoor and outdoor tests, discuss system performance and outline the challenges to be addressed next.

II. RELATED WORK

Research directions in legged locomotion include statically stable, dynamically stable, running and climbing robots, and can also be classified into bipedal (such as [5], [6]) and multi-pedal (>2 legs) robots (such as [7], [8]). In the following brief review, we focus on statically stable, multi-pedal robots developed for complex and challenging indoor or outdoor environments.

Statically stable legged robots range from smaller, highly mobile systems such as HECTOR [9] and Weaver [10] to multi-ton vehicles such as ASV [11], Ambler [12] and

COMET-IV [13]. Small vehicles such as RHex [14] and Messor-2 [15] do not have the range or payload capability required for long-distance traversal of difficult terrain, while large vehicles suffer from substantial power requirements and low speeds [4].

Hybrid designs that combine legs and wheels [16] can offer an interesting compromise between traversal capability and power efficiency, but are limited to operating on firm, open terrain and moderate slopes. BigDog [17] and its variants are four-legged robots that have demonstrated effective mobility in mild to moderate terrain. These vehicles have significant power requirements, however, and cannot traverse complex obstacle fields, fissures or non-solid terrain. Dante II [18] relied on a tether system to traverse a steep slope. Some concepts of amphibious robots have been explored (for an early example, see [19]), but today there are no truly multi-terrain legged robots that can traverse land, shallow water, and/or transition zones such as swamp, marsh or surf.

There is a significant body of research on flexible manipulators [20], [21], [22]. These are distributed parameter systems [23] that are far more complex to model than rigid manipulators. As a result, much of the work has concentrated on manipulators with small link deformations, planar single-link or dual-link manipulators, or manipulators operating in a gravity-free environment, all of which allow assumptions that greatly simplify some of the modeling and control problems.

Ultralight legged robots are largely a new area of research. An early, related concept was the venerable Odex-1 [24], which used a pantographic leg design. Few investigators have explored the use of flexibly deformable legs for robot locomotion; some of the work has been done in the context of hopping machines [25], but most of the interest has been in prosthetic legs with springs and energy storage (for an example, see [26]). More recently, the THALeR project [27] has developed a 10 ft tall, three-legged under-actuated robot platform that explores using the fewest number of actuators to achieve controlled locomotion.

III. TOWARDS ULTRALIGHT ROBOTS

Traditional approaches to robot design of manipulators, wheeled and legged robots usually emphasize structural stiffness of body and links and accurate actuated joints without uncontrolled compliance. This generally leads to systems with negligible or small deformations and with well-known kinematics and dynamics, enabling accurate and precise motion with relatively simple control systems. These designs tend, however, to be characterized by high mass/size ratios, high power requirements, and low payload to total system mass ratios.

In the Ultralight Robot approach we explicitly design for low mass, low power requirements and moderate to high speeds. This requires the use of lightweight materials and structures that may deform elastically under load, and to limbs and actuators that may be compliant in uncontrolled ways. We accept that these choices may lead to robots that will oscillate and sway during locomotion; significant uncertainties in state estimation, motion control and foot

placement; and the need for novel control and planning methods. We build on our research in stabilization of legged robots [28], impedance-based control [10], energy-informed gait control [29], and motion planning under uncertainty [30]. In summary, we accept substantially greater complexity in modelling, state estimation, and control of the robot in return for the significant advantages achieved in robot mass, speed, power consumption and payload capabilities that ULRs bring.

IV. THE MULTILEGGED AUTONOMOUS EXPLORER (MAX)

The long-term vision of our research is the development of large-scale, ultralight multi-legged robots able to achieve moderate speeds with modest power requirements, and capable of traversing complex and challenging 3D environments, both indoors and outdoors.

We have developed the first prototype of MAX (Multi-legged Autonomous Explorer) as a research prototype that allows us to address the core challenges of mechanism design, modelling, state estimation and control, and gait and motion planning faced by larger-scale, ultralight legged robots.

A. High-Level Specifications

The primary requirements for the design of MAX included:

- Very low mass to reduce power requirements
- Height of at least 2 m, when in a fully erect stance, to provide a higher vantage point for perceptual surveys of the area of operation
- Six-legged design for increased stability and redundancy
- Ability to step over obstacles at least 1 m tall
- Science payload capability of at least 10 kg
- Ability to negotiate standard door openings for traversal of buildings
- Initial target cruise speed of 1 m/s

B. Overall Design of MAX

The body of MAX is made of tubular aluminium, with a length, width and height of 1.2 m, 0.24 m and 0.17 m respectively. It houses the onboard avionics, as well as the batteries and the power distribution, communication, and safety systems.

MAX has been designed with 6 legs, allowing it to move in a variety of gaits while maintaining static stability. Six legs also provides added stability in the traversal of difficult or complex 3D terrain, as well as redundancy in case of leg failure. More legs might provide additional traversal capabilities in very rough terrain, but would significantly add to the mass and power budgets.

The legs are attached to the body frame and have 3 degrees of freedom (DOFs) each. The joints are arranged in a pan, tilt, tilt configuration (starting from the body) and are called the coxa, femur and tibia joints. The corresponding coxa, femur and tibia links have lengths of 0.08 m, 0.8 m

and 1.5 m, respectively. Each individual leg weighs approximately 4.5 kg. The choice of 3 DOFs for each leg allows (x, y, z) position control of the foot, which is desirable for traversal of complex 3D terrain. More joints per leg would allow for additional controllability of leg and foot motion, but were again deemed excessive due to mass requirements.

The body length of 1.2 m is less than would be required to allow all legs to swing through the full excursion of the coxa (pan) joints. However, it was chosen as a compromise between leg excursion and robot maneuverability in tight places.

When fully erect, MAX is 2.25 m tall, and has a maximum ground clearance of 2.0 m. When the body is resting on the ground, the legs splay out to 3.0 m, and when in a standard cruise stance (with the body lower than the knees) the vehicle is approximately 1.5 m tall and covers a rectangle of 2.4 m \times 2.1 m (Fig. 1). In a fully operational configuration (including batteries, but without the science payload) MAX weighs 59.8 kg.

C. Leg and Foot Design

As mentioned above, each leg has 3 DOFs in a pan, tilt, tilt configuration. The coxa (pan) joints use Dynamixel Pro H54-200-S500-R servo motors [31]. The torques and forces created from the legs are transferred to the body through these actuators, thus providing the torque required for propelling the robot forward.

In many legged robot designs, the actuators are positioned at the joints. However, in the case of the femur and tibia joints, the actuator masses and their positioning at the end of the coxa and femur links would significantly increase the torque requirements for the coxa and femur actuators. We chose instead to operate the femur and tibia joints using two linear actuators with push-pull rod systems that are fixed to the femur link (Fig. 2), and thereby significantly reducing actuator mass and overall torque requirements. The linear actuators used are Maxon RE35 90 W DC motors with EPOS2 50/5 motor controllers [32].

The femur and tibia actuators are mirror images of each other, simplifying the design of the robot. Each joint is moved by a carbon fibre push-pull rod that connects the slide of the linear screw to an attachment point on the output side of the joint. This approach provides significant joint torques and mass reduction, but limits the range and speed of the joint. The geometric configuration of the femur and tibia actuators, joints and link lengths was designed to provide enough torque to enable the robot to stand up from a sitting configuration (with the body resting on the ground). The femur and tibia joints have ASM PRDS27 absolute angle encoders at the pivot points, providing sensing at a 50 Hz rate through a CAN bus system [33].

The leg links are made of pultruded carbon fibre. The femur link has a length of 0.8 m between pivot points, and carries the linear actuator for the tibia joint. The tibia link is 1.5 m long and does not carry actuators.

The feet of the robot were designed to reduce ground impact forces, increase surface grip for motion and enable

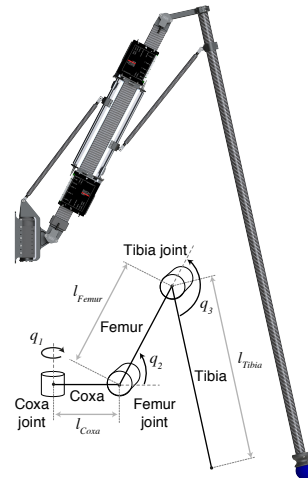


Fig. 2. Leg structure and naming convention.

measurement of contact forces. We currently use an interim solution, where the foot is made of a rubber sphere that is connected via a silicone tube to a pressure sensor located at the tibia joint. This avoids having electronic components on the foot, and enables the robot to walk through wet terrain. However, as the feet are pneumatic they are susceptible to puncture. We plan to transition to a new foot design and the use of waterproof force/torque sensors in the next upgrade of MAX.

D. Avionics

The avionics system for MAX includes (Fig.3):

- An embedded Intel i7 processor running Ubuntu and ROS.
- Two CAN buses, one for control of the Maxon linear actuators and the other for reading the ASM absolute angle encoders.
- An RS485 bus for control of the Dynamixel motors.
- A wireless router that provides a local area network and allows other systems to be integrated using either gigabyte Ethernet or WiFi.
- A remote operator station connected to MAX using the WiFi network and that also provides joystick control of the vehicle.
- Multiple redundant safety systems that allow wireless system shutdown in case of emergencies.

E. Power System

When conducting untethered operations, MAX is powered using two Lithium iron phosphate batteries in series, providing 24 V at 45 Ah. Power is provided to the subsystems of the robot using a power measurement and distribution module that in turn is controlled by the safety systems. In emergencies, this allows remote partial shutdown of individual subsystems or full system shutdown. When in the test bay, MAX uses a power tether.

F. Other Proprioceptive Sensors

Additional proprioceptive sensors on MAX include:

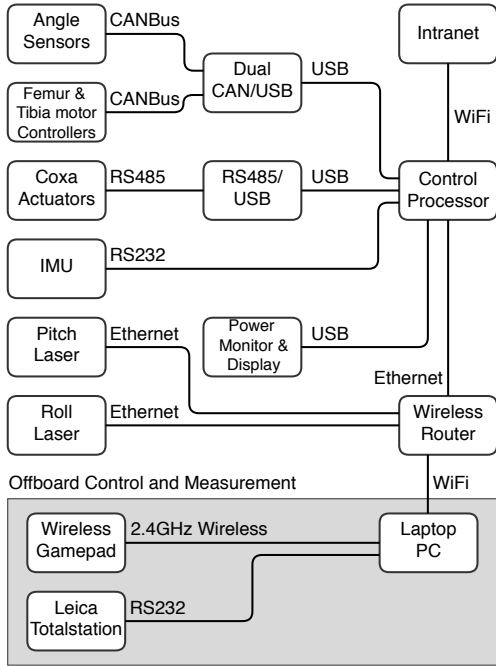


Fig. 3. MAX hardware system architecture.

- A SBG IG-500N IMU that provides a 9 DOF AHRS at 100 Hz, as well as GPS global position estimates.
- Two downward-facing Hokuyo UTM-30LX-EW lidars mounted on the belly of the vehicle, one with the scan direction aligned with the longitudinal axis and the other with the lateral axis of the robot. The lidars enable mapping of the terrain below the vehicle and provide accurate estimates of ground clearance.

V. CONTROL ARCHITECTURE

The control architecture of MAX has a hierarchical and modular structure. A simplified overview is shown in Fig. 4.

The Robot Locomotion Controller receives commanded body trajectories that come either from an operator using a control pad or from a Robot Trajectory Planner. Using one of the available gaits, it then computes the required leg trajectories to execute the body trajectory. The leg trajectories are executed by the Impedance-Based Leg Controllers, which send the corresponding control commands to the Joint Controllers for each leg, that are in turn executed by the Motor Controllers. The layers of the control architecture are discussed in more detail below. The system is implemented on top of ROS.

The first version of MAX's control architecture combines kinematics-based planning of body and leg motion with impedance-based control of the legs, but does not yet incorporate full dynamics-based body motion control. Although this is suboptimal for the control of a robot with significant dynamics and that oscillates and sways during locomotion, it was a deliberate choice that allowed us to investigate the performance of MAX using simpler legged locomotion control systems we developed earlier [28], [29], [10]. Within the ULR design paradigm, this also allowed us to assess to what extent swaying and oscillations could be tolerated

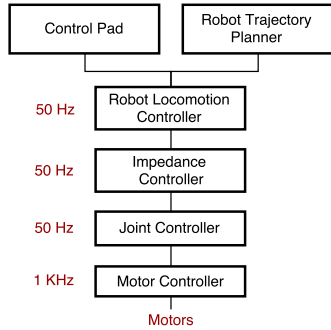


Fig. 4. Hierarchical structure of the control architecture with update rates.

in the system, and when it would become necessary to actively control them. The results obtained from the initial performance characterization experiments conducted with MAX (Section VI) are essential for system identification and for the subsequent development of a hybrid dynamics-based control system for MAX.

A. Motor Controllers

The distal leg joints are controlled using CANopen joint angle sensors and motor controllers. The system is partitioned into two CANopen networks with the joint angle sensors separated from the motor controllers. A commercial implementation of the CANopen protocol (the CMI library) was used to speed up the development of the ROS drivers. The drivers used standard ROS JointState messages to communicate the joint angles obtained from the sensors. The motor drivers were also written to use JointState messages for reporting the motor state and for providing the joint reference values for the motor controllers. The design of the joint controllers proved to be challenging and is detailed in the next section.

B. Joint Controllers

The function of the joint controllers is to track accurately the different reference joint angles computed by the impedance and high-level walking controllers, as described in the subsections below. This layer is therefore responsible for controlling the motion of the 18 joints of MAX, and includes two different types of joint controllers: standard PID controllers for the coxa joints (using rotational actuators), and hybrid feedforward-feedback controllers for the femur and tibia joints (using linear actuators).

The coxa joints use Dynamixel actuators and controllers (Section IV-C) which already include PID loops that can be tuned. The other joints are actuated using linear actuators (section IV-C), and controlling them turned out to be very challenging. The dynamics of the system relating the joint angles $q_i(t)$ to their control input $u_i(t)$ (motor speed) is highly nonlinear and complex. Several experiments showed that implementing simple PID controllers resulted in system instability and substantial oscillations that are amplified by the flexibility and elasticity of the joints and the vehicle.

A simple but effective control strategy was developed to overcome these issues and ensure accurate tracking while

minimising oscillations. The controllers used for the femur and tibia joints are composed of two cascaded loops (position loop and velocity loop) with feedforward and feedback terms. Specifically, the joint controller is given by (Fig. 5):

$$u_i = pid(\dot{q}_{i\text{ref}}, \dot{q}_i) + g(\dot{q}_{i\text{ref}}, q_i) \quad (1)$$

$$\dot{q}_{i\text{ref}} = pid(q_{i\text{ref}}, q_i) + f(q_i) \quad (2)$$

where $u_i(t)$ is the computed reference motor speed sent to the motor controller discussed earlier, $pid(\cdot)$ is the standard PID function, $g(\cdot)$ is a nonlinear function that implements the feedforward term and $f(\cdot)$ is a first-order derivative filter. For better performance, the joint controllers have been augmented by adaptive deadband and smoothing filters as shown in Fig. 5.

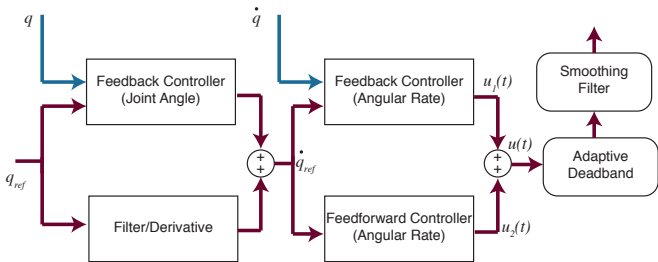


Fig. 5. Hybrid controller structure for the femur and tibia joints which use linear actuators.

Tests showed that the Joint Controller achieved excellent results in controlling the joint angles to track desired values provided by the Vehicle Motion Controller (Fig. 6).

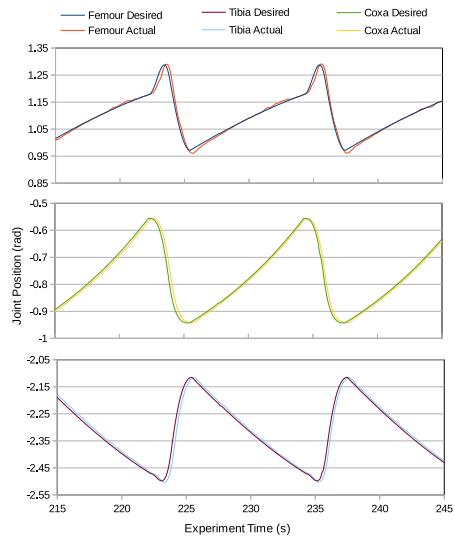


Fig. 6. Typical tracking example of coxa, femur and tibia joints of front left leg during two step cycles of the Ripple gait.

C. Impedance-Based Leg Controllers

We use an impedance-based formulation for control of leg motions through gait cycles, modified from the one described in [10]. The controller transforms the force at the foot tip,

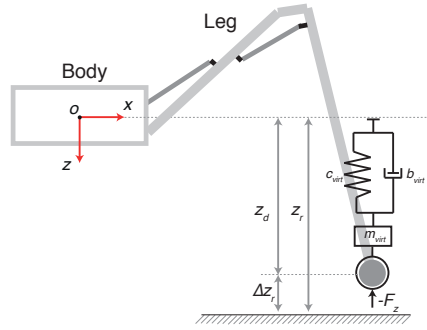


Fig. 7. The equivalent model of the impedance controller is a second order mechanical system attached to the foot tip.

measured by pressure or force sensors, into a displacement along the vertical axis of the body. This allows the robot to ensure that foot contact with the terrain has been established and to distribute the forces on the legs while walking through uneven terrain. A virtual mass m_{virt} , virtual stiffness c_{virt} and virtual damping element b_{virt} define the dynamic behavior in the z direction. The second order system is given by

$$-F_z = m_{virt}\ddot{\Delta z}_r + b_{virt}\dot{\Delta z}_r + c_{virt}\Delta z_r \quad (3)$$

This virtual second order mechanical system reacts to measured ground forces and adapts the desired foot position and exerted force. The adapted foot position becomes $z_d = z_r - \Delta z_r$. The displacements Δx_r and Δy_r are set to zero in order to keep the foot tip stiff in the x and y directions. The equivalent model of the impedance controller in Cartesian space is shown in Fig. 7.

D. Robot Locomotion Controller

The robot locomotion controller translates commanded body trajectories into commanded leg motions, computed using a kinematic model of the vehicle. The commanded body trajectories can come either from a human operator using a control pad, or from a higher-level robot trajectory planning system.

The commanded robot body speed is achieved by controlling the leg stride length and frequency. In general, stride frequency is kept equal for all legs, which keeps the stride pattern synchronised across the legs. The stride length and direction, together with a global stride phase, are passed into a foot cycle generator which moves the foot along a predefined cyclic curve that includes swing and stance states. Because of system flexing during locomotion, the body of MAX tends to sag when legs are lifted off the ground. The locomotion controller also adjusts target body pose to compensate for this body sag.

The initial gaits selected for testing on MAX are Wave, Amble, Ripple and Tripod. These are defined in Fig. 8, which shows the step cycle timing differences between each of the gaits. Experimental performance results obtained using different gaits are shown in the next section.

VI. FIELD TESTS AND EXPERIMENTAL PERFORMANCE

In the initial performance characterization experiments conducted with MAX, the parameters measured included

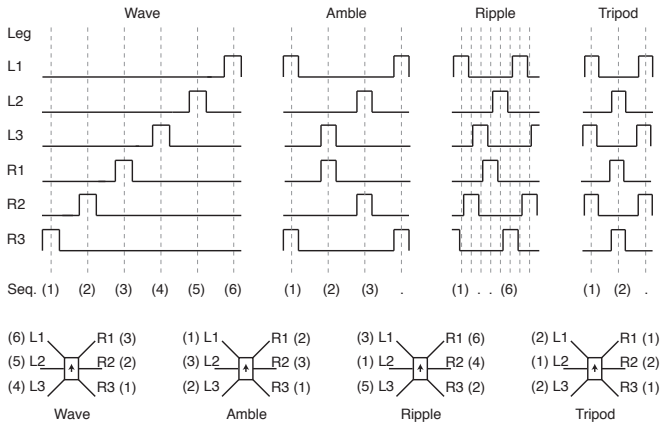


Fig. 8. Gait timing diagrams for the four gaits tested on MAX: Wave, Amble, Ripple and Tripod. The sequence number shows the order in which the legs move. L1-L3 refers to legs on the left and R1-R3 refers to legs on the right.

achievable body velocity, vehicle stability, power consumption and cost of transport for various gaits; magnitude and frequency of body oscillations and swaying; and other performance metrics. The results are essential for system identification and for the subsequent development of a hybrid dynamics-based control system for MAX. This section summarizes some of our results.

Indoor experiments were conducted in a large test bay with a relatively flat concrete surface 9. These included having MAX repeatedly traverse a distance of approximately 8 m, each time using one of the four gaits discussed earlier (Section V-D): the Wave, Amble, Ripple and Tripod gaits. For each gait, a target velocity was chosen that represented a tradeoff between speed and safety.

Outdoor experiments were conducted in a large open paved surface, and in a wooded area where MAX transitioned from a concrete surface to a grassy area with a very mild slope.

During both indoor and outdoor tests, the speeds were kept deliberately low for safety reasons, and hence the results discussed below do not represent the maximum performance that can be achieved for each gait. Nevertheless, they provide an initial characterization of robot performance.

A. Indoor Tests

During indoor tests, MAX walked repeatedly along an 8 m trajectory, using its four different gaits. A Leica Total Station laser tracking system was used to estimate the position of the robot's body in an absolute reference frame, using a reflector prism mounted on the body. During these tests, MAX was attached to an overhead gantry crane via a safety harness, to ensure the safety of the robot in case of major failures.

The avionics IMU was used to measure body oscillations and swaying during locomotion. Additionally, several external cameras were used to record the experiments. An onboard camera mounted at the back of the vehicle and looking forward provided an additional record of the vehicle actions.

The locomotion performance of MAX for various gaits is shown in Fig. 10. Total displacement was computed along



Fig. 9. MAX in the indoor test bay. In the front is a Velodyne lidar used for 3D SLAM.

the trajectory executed by the robot, as measured by the Total Station. In the context of our experimental setup, the Wave gait was the slowest, while the Ripple gait proved to be the fastest. Note that the Ripple gait experiment required a brief stoppage around the 3 m mark, to allow the impedance controller to re-balance the foot positions because of changes in the terrain. This was corrected for in the summary results shown in Table I.

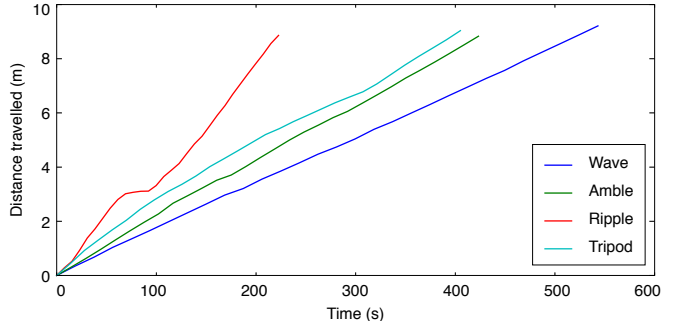


Fig. 10. Distance traveled by the robot as a function of time along trajectories tracked by the Leica Total Station. Tests for four gaits are shown.

These experiments were performed in order to evaluate the performance characteristics of MAX under differing stance parameters, control parameters and gait. The preliminary results are informative, but cannot be generalized to what the robot's performance will be when it is exercised at full speed.

Measuring the oscillations and swaying induced by different gaits and speeds is essential to assess the stability of the hexapod. The phase plane plots in Fig. 11 use data collected from the avionics IMU, and show that the Ripple gait induced significantly higher oscillations than the other

gaits. The Wave gait induced a slight drift of MAX to the right during locomotion when no heading correction was used; this is due to the sequencing pattern of the legs and minor geometric variations between the legs.

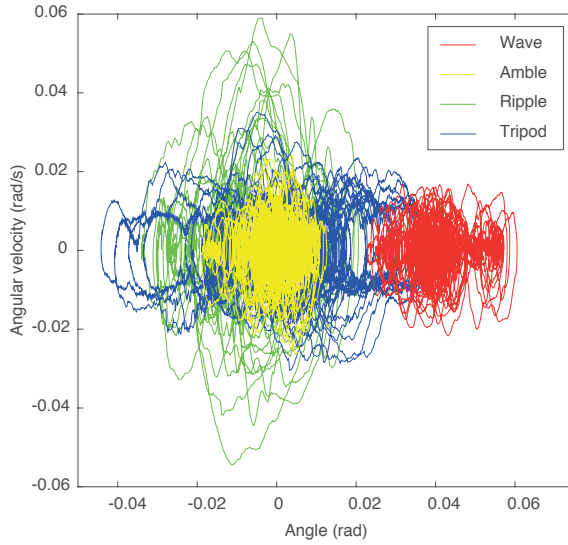


Fig. 11. Combined phase plane plots for the four different gaits used, showing the stability of the platform in each case. The data was obtained from the avionics IMU.

Another important performance metric is the average power consumption for different gaits and speeds. Power measurements are obtained from onboard battery voltage and current monitors. For the speeds and gaits shown in Fig. 10, the power consumption is shown in Fig. 12 and is summarized in Table I. Overall, the average power consumption stayed within 100-150 W. In the average, the Wave gait had the lowest power consumption while the Ripple gait had the highest. It should again be emphasized that these results are heavily dependent on the details of our experimental setup.

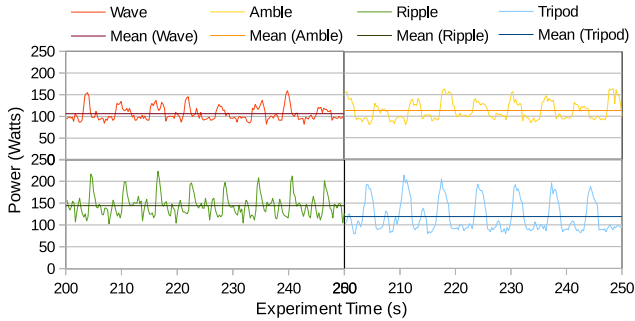


Fig. 12. Typical power consumption of MAX for different gaits and over the same time length.

From the speed and power consumption data, we can calculate the dimensionless energetic cost of transport (CoT), which is a very useful metric in evaluating MAX's locomotion efficiency for different gaits and for comparison with other walking robots and living creatures [34], [29]. The overall cost of transport \bar{e} over a traversed distance is given

by

$$\bar{e} = \frac{\frac{1}{n} \sum_{i=1}^n V_i I_i}{mg \frac{\Delta x}{\Delta t}} \quad (4)$$

where V_i and I_i are battery voltage and current draw measured at time step i , m is the mass, g is the gravitational acceleration, and Δt is the time taken to travel distance Δx . n is the number of time steps considered. This metric includes mechanical energy, dissipated heat, and other losses (e.g. friction). Table I summarizes speed, power consumption and cost of transport for different gaits.

TABLE I
ENERGETIC PERFORMANCE OF GAITS

Gait	Mean Speed (m/s)	Power Consumption (W)	Cost of Transport
Wave	0.017	107.4 ± 16.6	10.87
Amble	0.021	113.9 ± 22.5	9.27
Ripple	0.047	140.7 ± 23.5	5.08
Tripod	0.022	120.4 ± 36.8	9.23

B. Outdoor Tests

In addition to indoor experiments, which were undertaken to evaluate the performance of MAX, we also ran some outdoor experiments in less controlled testing conditions, and without the overhead fail-safe gantry crane. The tests were conducted in a large outdoor industrial courtyard with paved surfaces, and in a wooded area where MAX transitioned from a concrete surface to a grassy area with a very mild slope.

In the industrial courtyard several gaits were again tested on MAX, as well as "on the fly" transitions between gaits. The vehicle performance was similar to the results obtained from the indoor tests discussed above.

In the test conducted in the wooded area, MAX used a Wave gait to walk along a pedestrian walkway and transition to a grassy area with a very mild upward slope (Fig. 1). While there were no significant differences in overall power consumption for the two surfaces (Fig. 13), as the vehicle transitioned to a mild slope the average power had a clear oscillation pattern (starting around 450 s) that could potentially be caused by the rear legs pushing the vehicle up.

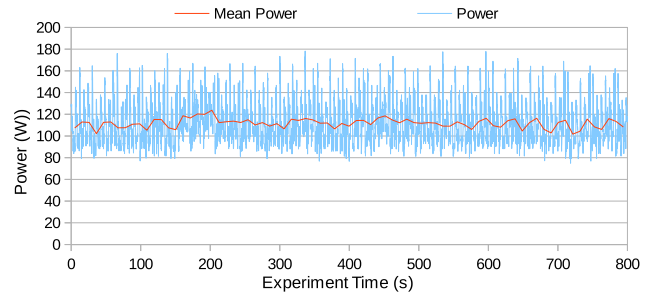


Fig. 13. Power consumption of MAX during outdoor test with transition from paved to grassy surface.

VII. CONCLUSIONS

In this paper we introduced MAX, our first prototype of an Ultralight Legged Robot. MAX has a fully erect height of 2.25 m and a weight of 59.8 kg. In initial tests that were conducted at very slow speeds for safety reasons, the power consumption across various gaits stayed within a range of 107 – 141 W, and the cost of transport varied between 5.08 and 10.87. We compared MAX with the size and performance data for a large number of legged robots provided in [4]. Scaling other larger-scale robots to sizes similar to our vehicle, we found that MAX is roughly 5 to 20 times lighter than other designs, and has a cost of transport comparable with that of significantly smaller vehicles.

The experimental results we presented are representative of MAX's performance at very low speeds, but are not indicative of its performance at maximum achievable speeds. The next steps in our research include a) the development of an active body stabilization system, b) the subsequent execution of a more extensive set of experiments with MAX operating at top speeds for its various gaits, c) performing long-distance trials in moderately difficult terrain, and d) a more extensive and detailed comparison of the performance achieved by MAX with that of other comparable legged robots.

VIII. ACKNOWLEDGMENTS

The authors would like to thank Adrian Bonchis, Jorge Diosdado Borrego, Brett Wood, Les Overs and Stephen Brosnan for their contributions to the design and development of MAX and its onboard control systems.

REFERENCES

- [1] US Army, "Corps of Engineers Wetlands Delineation Manual," Wetlands Research Program, US Army, Tech. Rep. Y-87-1, 1987.
- [2] ———, "Terrain Analysis," Washington, DC, Tech. Rep. Field Manual No. 5-33, July 1990.
- [3] D. C. Kar, K. K. Issac, and K. Jayarajan, "Gaits and Energetics in Terrestrial Legged Locomotion," *Mechanism and Machine Theory*, vol. 38, 2003.
- [4] F. Tedeschi and G. Carbone, "Design Issues for Hexapod Walking Robots," *Robotics*, no. 3, pp. 181–206, 2014.
- [5] Honda Motor Corporation, "ASIMO: The Honda Humanoid Robot," Honda Motor Co., Ltd., Japan, Tech. Rep., September 2007.
- [6] Boston Dynamics, "Atlas - The Agile Anthropomorphic Robot," Boston Dynamics, Boston, USA, URL:, 2016. [Online]. Available: http://www.bostondynamics.com/robot_Atlas.html
- [7] A. Roennau, G. Heppner, M. Nowicki, and R. Dillmann, "LAURON V: A versatile six-legged walking robot with advanced maneuverability," in *IEEE/ASME International Conference on Advanced Intelligent Mechatronics (AIM)*, 2014, pp. 82–87.
- [8] D. J. Hyun, S. Seok, J. Lee, and S. Kim, "High speed trot-running: Implementation of a hierarchical controller using proprioceptive impedance control on the MIT Cheetah," *The International Journal of Robotics Research*, vol. 33, no. 11, pp. 1417–1445, 2014.
- [9] A. Schneider, J. Paskarbeit, M. Schaeffermann, and J. Schmitz, "HECTOR, a New Hexapod Robot Platform with Increased Mobility - Control Approach, Design and Communication," in *Advances in Autonomous Mini Robots: Proceedings of the 6-th AMiRE Symposium*, U. Rückert, S. Joaquin, and W. Felix, Eds. Berlin: Springer Verlag, 2012, pp. 249–264.
- [10] M. Bjelonic, N. Kottege, and P. Beckerle, "Proprioceptive control of an over-actuated hexapod robot in unstructured terrain," in *Proceedings of the IEEE/RSJ International Conference on Intelligent Robots and Systems (IROS)*, 2016.
- [11] K. J. Waldron and V. J. Vohnout, "Configuration Design of the Adaptive Suspension Vehicle," *International Journal of Robotics Research*, vol. 3, no. 2, Summer 1984.
- [12] J. Bares and W. L. Whittaker, "Walking Robot With a Circulating Gait," in *IEEE/RSJ International Conference on Intelligent Robots and Systems (IROS)*. IEEE/RSJ, July 1990.
- [13] K. Nonami, R. K. Barai, A. Irawan, and M. R. Daud, "Force-based locomotion control of hexapod robot," in *Hydraulically Actuated Hexapod Robots*. Springer, 2013, pp. 141–167.
- [14] U. Saranli, M. Buehler, and D. Koditschek, "RHex: A Simple and Highly Mobile Hexapod Robot," *International Journal of Robotics Research*, vol. 20, no. 7, 2001.
- [15] D. Belter and K. Walas, "A Compact Walking Robot Flexible Research and Development Platform," in *Recent Advances in Automation, Robotics and Measuring Techniques*, ser. Advances in Intelligent Systems and Computing, R. Szewczyk, C. Zieliński, and M. Kaliczyńska, Eds. Springer, 2014, vol. 267, pp. 343–352.
- [16] B. H. Wilcox, "ATHLETE: A Cargo and Habitat Transporter for the Moon," in *IEEE Aerospace Conference*, Big Sky, MT, March 2009.
- [17] M. H. Raibert *et al.*, "BigDog, the Rough-Terrain Quadruped Robot," in *17th IFAC World Congress*, South Korea, July 2008.
- [18] J. Bares and D. S. Wettergreen, "Dante II: Technical Description, Results, and Lessons Learned," *International Journal of Robotics Research*, vol. 18, no. 7, July 1999.
- [19] R. Harkins *et al.*, "Design and Testing of an Autonomous Highly Mobile Robot in a Beach Environment," in *Proceedings of the WCECS 2008*, San Francisco, CA, October 2008.
- [20] R. Robinett *et al.*, *Flexible Robot Dynamics and Control*. New York: Kluwer, 2002.
- [21] B. Subudhi and A. S. Morris, "Dynamic Modelling, Simulation and Control of a Manipulator with Flexible Links and Joints," *Journal of Robotics and Autonomous Systems*, no. 41, 2002.
- [22] M. Tokhi *et al.*, "Flexible Manipulators – An Overview," in *Flexible Robot Manipulators*, M. Tokhi and A. Azad, Eds. London: IET Press, 2008.
- [23] Y. Gao and F. Wang, "A Comprehensive Study of Dynamic Behaviors of Flexible Robotic Links: Modeling and Analysis," in *Advanced Studies of Flexible Robotic Manipulators*, F. Y. Wang and Y. Gao, Eds. NJ: World Scientific Publishing, 2003.
- [24] T. Bartholet, "Odetics Makes Great Strides," *Nuclear Engineering*, vol. 31, no. 381, April 1986.
- [25] H. Brown and G. Zeglin, "The Bow Leg Hopping Robot," in *Proceedings of the IEEE International Conference on Robotics and Automation*, May 1998.
- [26] R. D. Bellman, M. A. Holgate, and T. G. Sugar, "SPARKy 3: Design of an Active Robotic Ankle Prosthesis with Two Actuated Degrees of Freedom Using Regenerative Kinetics," in *Proc. Of the 2nd IEEE RAS & EMBS International Conference on Biomedical Robotics and Biomechatronics*, 2008.
- [27] J. Webb, A. Leonessa, and D. Hong, "Gait Design and Gain-Scheduled Balance Controller of an Under-Actuated Robotic Platform," in *Proceedings of the 2015 IEEE/RSJ International Conference on Intelligent Robots and Systems (IROS)*. Hamburg, Germany: IEEE/RSJ, 2015.
- [28] M. Hoerger, A. Elfes, N. Kottege, T. Bandyopadhyay, and P. Moghadam, "Real-time Stabilisation for Hexapod Robots," in *International Symposium on Experimental Robotics (ISER)*, Marrakech and Essaouira, Morocco, June 2014.
- [29] N. Kottege, C. Parkinson, P. Moghadam, A. Elfes, and S. P. Singh, "Energetics-informed hexapod gait transitions across terrains," in *IEEE International Conference on Robotics and Automation (ICRA)*, 2015.
- [30] M. Hoerger, H. Kurniawati, A. Elfes, and T. Bandyopadhyay, "Linearization in Motion Planning under Uncertainty," in *12th International Workshop on the Algorithmic Foundations of Robotics (WAFR)*, vol. Accepted for publication., San Francisco, CA, December 2016.
- [31] Robotis, "Robotis Dynamixel Pro, URL:" 2014. [Online]. Available: http://www.robotis.com/xe/DynamixelPro_en
- [32] Maxon MotorsURL:, 2016. [Online]. Available: <http://www.maxonmotor.com/maxon/view/content/index>
- [33] ASM Automation SensorikURL:, 2016. [Online]. Available: <http://www.asm-sensor.com>
- [34] J. Nishii, "An analytical estimation of the energy cost for legged locomotion," *Journal of theoretical biology*, vol. 238, no. 3, pp. 636–645, 2006.